Journal of The Electrochemical Society, **148** (11) A1279-A1286 (2001)
0013-4651/2001/148(11)/A1279/8/$7.00 © The Electrochemical Society, Inc.

Synthesis and Cathodic Properties of $LiCo_{1-y}Rh_yO_2$ $(0 \leqslant y \leqslant 0.2)$ and $LiRhO_2$

S. Madhavi,[a] G. V. Subba Rao,[b,*] B. V. R. Chowdari,[b,c,z] and S. F. Y. Li[a,b]

[a]*Department of Chemistry, National University of Singapore, Singapore 119260*
[b]*Institute of Materials Research and Engineering, Singapore 117602*
[c]*Department of Physics, National University of Singapore, Singapore 119260*

Compounds of the formula $LiCo_{1-y}Rh_yO_2$ ($0.0 \leqslant y \leqslant 0.20$ and $y = 1.0$) have been synthesized by high temperature solid-state reaction and characterized by X-ray diffraction (XRD), X-ray photoelectron spectroscopy, and infrared spectroscopy. Single-phase materials were obtained for $y \leqslant 0.10$ and $y = 1.0$ as observed by XRD. However, IR and electrochemical data indicate that the true solid solubility may be $y \leqslant 0.05$. Their cathodic behavior in coin cells with Li metal as anode and a liquid electrolyte has been examined. Cyclic voltammograms and galvanostatic charge/discharge curves show that for $y = 0.05$, the phase transformation occurring at $x = 0.5$ in $Li_{1-x}CoO_2$ is suppressed and the deintercalation voltage is decreased. The compositions with $y = 0.05$ and 0.10 show improved cathodic behavior and discharge capacity retention compared to $LiCoO_2$ ($y = 0$) at 0.14C rate in the voltage range 2.7-4.3 V up to 18 cycles. Electrochemical studies on $LiRhO_2$ show that phase transitions occur on charge/discharge cycling (varying x in $Li_{1-x}RhO_2$) in the voltage window 3.2-3.7 V and these are reversible. This compound shows an initial charge capacity of 162 mAh/g when charged to 4.0 V (*vs.* Li metal), corresponding to $x = 0.85$ in $Li_{1-x}RhO_2$. After an initial loss of 40 mAh/g in capacity, the discharge capacity retention corresponds to 90% after 18 cycles with respect to the initial discharge capacity in the voltage window, 2.7-4.0 V.
 [DOI: 10.1149/1.1410968]

Manuscript submitted January 30, 2001; revised manuscript received June 20, 2001. Available electronically October 12, 2001.

Commercial lithium-ion batteries presently use $LiCoO_2$ as the cathode material due to its high performance characteristics.[1,2] $LiNiO_2$[3-5] and $Li(Ni_{1-y}Co_y)O_2$[6-11] are now being investigated extensively as prospective high capacity cathodes. These mixed oxides possess a hexagonal layer structure and contain ordered array of Li and Co ions sandwiched between the oxide ion layers. The metal ions adopt an octahedral oxygen coordination and the unit cell contains three formula units of $LiCoO_2$. They are usually referred to as O3 type or α-$NaFeO_2$-type with the space group, $R\bar{3}m$. Isostructural analogues with other transition metals, viz., $LiCrO_2$, $LiRhO_2$, $LiFeO_2$, and $LiMnO_2$ are known. While $LiMO_2$ with M = Co, Ni, Cr, and Rh can be prepared by a high temperature solid-state reaction in air or oxygen; $LiFeO_2$[12-15] and $LiMnO_2$[15-19] can only be prepared under hydrothermal or soft-chemistry techniques. The latter two compounds have received wide attention for their cathodic behavior because of the obvious cost considerations, containing cheap and environmentally friendly iron and manganese oxides.

In addition to the nickel dopant mentioned above, several 3d transition elements like Mn,[20] Cr,[21] Fe,[22] and nontransition metals like B,[23] Al,[24-27] and Mg[28] have been studied extensively as dopants in $LiCoO_2$ with the aim of improving its electrochemical characteristics in terms of cycling efficiency, intercalation voltage, and cost reduction. A wealth of information is now available not only with respect to the cathodic behavior but also on the physical properties of these doped $LiCoO_2$ in the pristine as well as in the charged (Li deintercalated) state.[7,10,29-32] Theoretical *ab initio* calculations by Ceder *et al.*[24,33] have indicated that the replacement of Co in $LiCoO_2$ by other 3d transition elements (M = Ti, V, Mn, Ni) decreases the average intercalation voltage, whereas a replacement by a nontransition metal like Al increases the intercalation voltage for a given value of x in $Li_{1-x}CoO_2$. However, the imposed condition was that these $LiMO_2$ compounds must exist in the α-$NaFeO_2$ structure. This prediction has been verified experimentally in the case of solid solutions $Li(Co_{1-y}Al_y)O_2$, $y \leqslant 0.5$ by Ceder *et al.*,[24] and several others.[25-27] Since $LiCoO_2$ and $LiNiO_2$ form complete solid solutions, it is expected that $LiCoO_2$ and $LiRhO_2$ may also form solid solutions because all these compounds are isostructural and can be synthesized in air or oxygen. The effect of a Rh-dopant on the electrochemical properties of $LiCoO_2$ has not yet been reported. Synthesis and preliminary electrochemical behavior of $ARhO_2$ (A = Li, Na, and K) have been reported by Mendiboure *et al.*[34] However, detailed electrochemical study on $LiRhO_2$ is lacking. Presently, we report the synthesis, characterization, and cathodic properties of the Rh-doped $LiCoO_2$ and $LiRhO_2$.

Experimental

Compounds of the type $LiCo_{1-y}Rh_yO_2$ ($0.0 \leqslant y \leqslant 0.20$) were synthesized by heating stoichiometric mixtures of high purity raw materials, Co_3O_4 (Merck), $Rh(NO_3)_3 \cdot 2H_2O$ (Alfa), and LiOH (Merck) at 850°C for 20 h in air followed by slow cooling (1°C min^{-1}). $LiRhO_2$ was synthesized by heating stoichiometric mixtures of rhodium and lithium salts as above at 900°C for 24 h in flowing oxygen atmosphere followed by slow cooling (1°C min^{-1}). Powder X-ray diffraction (XRD) was used to identify the crystalline phases (Siemens D5005, Cu $K\alpha_1$ radiation). The XRD patterns were indexed and lattice parameters calculated using least squares fitting of the *d* spacings and Miller indices (*hkl*). Midinfrared spectral studies in the range of 400-4000 cm^{-1} were done using a Fourier transform infrared (FTIR) Bruker Equinox 55 system with a spectral resolution of 4 cm^{-1}. Fine powders of the compounds were mixed with KBr and pressed to give translucent pellets. X-ray photoelectron spectroscopy (XPS) studies were carried out on the powder samples using a VG electron spectroscopy for chemical analysis lab MKII spectrometer. Samples were loaded by dusting the sample powder on to a polymeric-based adhesive tape stuck on the sample holder. All spectra were recorded using an X-ray source (Mg $K\alpha_1$ radiation) with a scan range of 1200-0 eV binding energy. High-resolution spectra were recorded in selected energy ranges of interest. The collected XPS spectra were analyzed using XPS Peak 95 version 3.1 software peak fitting program.

The galvanostatic charge/discharge cycling tests were carried out using two electrode coin cells with lithium metal foil as the anode. A 1:1 (v/v) mixture of ethylene carbonate (EC) and dimethyl carbonate (DMC) containing 1 M $LiPF_6$ was used as the electrolyte (Merck). The cathodes were made up of the oxide material, Super P carbon black as the conducting additive and polyvinylidene fluoride (PVDF) binder (in the weight ratio 80:10:10) in *n*-methylpyrrolidinone (NMP) solvent and were mixed to form a uniform slurry. Electrodes were fabricated by coating the above

* Electrochemical Society Active Member.
z E-mail: phychowd@nus.edu.sg

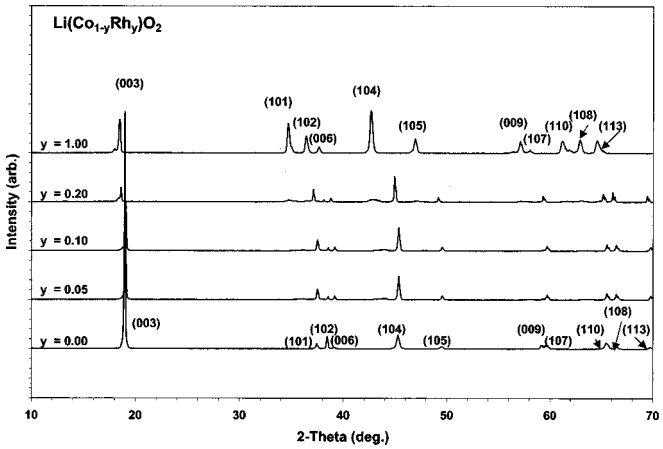

Figure 1. XRD patterns of the compounds, $Li(Co_{1-y}Rh_y)O_2$. *y* values and (*hkl*) Miller indices are indicated. Cu Kα radiation.

slurry onto an Al foil (25 μm thick) using a paint applicator and drying it in an air oven at 80°C to evaporate the solvent. The foil was then pressed between stainless steel rollers and dried in a vacuum oven to ensure that the electrode is free from moisture and solvent. The foil was then cut into circular strips of 16 mm diam. Coin-type test cells (size 2016) were assembled using polypropylene (Celgard) as the separator in an argon-filled dry box (MB150B-G, MBraun, USA) which maintains O_2, H_2O contents at <0.1 and <0.02 ppm, respectively. The open circuit voltage (OCV) of freshly fabricated cells with $LiCoO_2$ cathode was around 3.0-3.5 V, while that with $LiRhO_2$ cathode was around 3.0-3.2 V. The cathode active material in the coin cells is in the range of 10-15 mg and currents used for galvanostatic cycling are in the range of 0.05-0.25 mA. The charge/discharge tests and cyclic voltammograms were performed using computer controlled multichannel battery testing units (Bitrode, USA; Macpile, Biologic, France). The freshly fabricated cells were aged for 24 h before the electrochemical tests to ensure equilibration and soaking of cathode in the electrolyte.

Results and Discussion

Characterization by XRD, FTIR, and XPS.—The XRD patterns of $LiCo_{1-y}Rh_yO_2$ ($0.0 \leqslant y \leqslant 0.10$) showed the formation of single phase with a well-defined rhombohedral-hexagonal layer structure. No impurity phases are seen in this range of doping (Fig. 1). However, the XRD pattern of the $y = 0.20$ compound showed in addition to the peaks due to the desired phase, impurity peaks due to $LiRhO_2$ indicating that the solubility of Rh is less than 0.20 under the synthesis conditions presently employed. The XRD pattern of $LiRhO_2$ showed only barely detectable impurity peaks, which did not correspond to Rh_2O_3 or Li_2CO_3. During the least squares fitting of the $LiCo_{1-y}Rh_yO_2$ ($y = 0.20$) and $LiRhO_2$ care was taken to exclude the extraneous impurity peaks. The hexagonal lattice parameters (*a* and *c*) are listed in Table I. The values for $LiCoO_2$ are in very good agreement with those reported by Delmas *et al.*[6] and Saadoune and Delmas.[7] The *a* and *c* parameters of $LiRhO_2$ ($y = 1.0$) are also in accordance with the values reported ($a = 3.018$, $c = 14.20$ A) by Mendiboure *et al.*[34] Substitution of Rh at the Co site in $Li(Co_{1-y}Rh_y)O_2$ is expected to increase both *a* and *c* parameters if a Vegard's law-type behavior is obeyed, since the ionic radius of Rh^{3+} ion (0.665A) is larger than that of Co^{3+} ion (0.545 A; octahedral coordination; low spin state).[35] Our results show that while the *a* parameter follows the expected trend (with the exception of composition with $y = 0.1$), the *c* parameter decreases up to $y = 0.1$ and then shows an increase for $y = 0.2$. The reason for this behavior is not clear at present but it is possible that covalency effects play a role. We note that c/a corresponds to the metal-metal interlayer distance and covalency effects have been invoked by Saadoune and Delmas[7] to explain the behavior of *a* and *c* parameters in their study on the solid solutions, $LiNi_{1-y}Co_yO_2$ ($0 \leqslant y \leqslant 1.0$). As can be seen from Table I, the c/a ratio shows a smooth variation with *y* similar to that noted by the group of Delmas.[6,7]

It may be pointed out that since the ionic radius of Rh^{3+} is closer to that of Li^+ (0.76 A; octahedral coordination)[35] as compared to the ionic radius of Co^{3+}, there is a possibility of cation disorder in both $LiCo_{1-y}Rh_yO_2$ ($y = 0.1, 0.2$) and $LiRhO_2$ in the sense that some Li and Rh ions can interchange their positions in the respective layers. Theoretical calculations by Wu *et al.*[36] have shown that the α-$NaFeO_2$ structure can exist only if the radius ratio ($RR = r_M^{3+}/r_{Li}^{+}$) is <0.90. For $RR \geqslant 0.90$, cation disorder can occur, finally leading to a disordered rock salt structure. For M = Rh and Co, the RR values are 0.875 and 0.717, respectively, and thus we may expect cation disorder in $LiRhO_2$ and for $y > 0.1$ in $LiCo_{1-y}Rh_yO_2$. We have not done a Rietveld analysis of the observed powder XRD patterns, but an approximate indication of cation disorder can be discerned from the c/a and the relative intensity ratio (RIR) of the (003) and (104) lines in the XRD patterns (RIR = I(003)/I(104)). For a cation-disordered rock salt structure, we know that the c/a ratio should be $4.899(\sqrt{24})$. As seen from Table I, the c/a value for $LiRhO_2$ is 4.801, indicating the existence of cation disorder in the lattice. For $y = 0.1$ and $y = 0.2$, even though the c/a ratio is >4.899, the possibility of slight cation disorder exists.

Table I. Structural, IR, and cathodic capacity data of the compounds $Li(Co_{1-y}Rh_y)O_2$ ($0 \leqslant y \leqslant 0.20$ and $y = 1.0$).

y	Hexagonal lattice parameters, A				FTIR bands, cm^{-1}			Cathodic capacity (mAh/g)[a]		
	a (±0.002)	*c* (±0.005)	*c*/*a*	RIR[b]				Initial charge	Initial discharge	Discharge capacity retention 1st-18th cycle (%)
0.0 ($LiCoO_2$)	2.816	14.08	5.000	2.67	550 (537; 539)[d]	610-620 (b)[c] (595; 602)	655 (sh) [653 (sh)]	171	156	74
0.05	2.818	14.07	4.993	1.78	530	595-615 (b)	650 (sh)	170	135	91
0.10	2.812	14.00	4.979	1.82	525	595; 625	650 (sh)	161	144	86
0.20	2.841	14.04	4.942	0.61	515; 550	595; 625	650 (sh)	-	-	-
1.0 ($LiRhO_2$)	2.958	14.20	4.801	0.85 [1.11][e]	525-555 (b)	600 (sh)	-	162	122	90

[a] Voltage window: 2.7-4.3 V for $y \leqslant 0.1$ and 2.7-4.0 V for $y = 1.0$. Current rating, 0.14C.
[b] Relative intensity ratio of (003) and (104) lines in the XRD pattern.
[c] (b) broad, (sh) shoulder.
[d] Values in parentheses are for $LiCoO_2$ taken from Ref. 40, 41.
[e] Value in bracket is from Ref. 37.

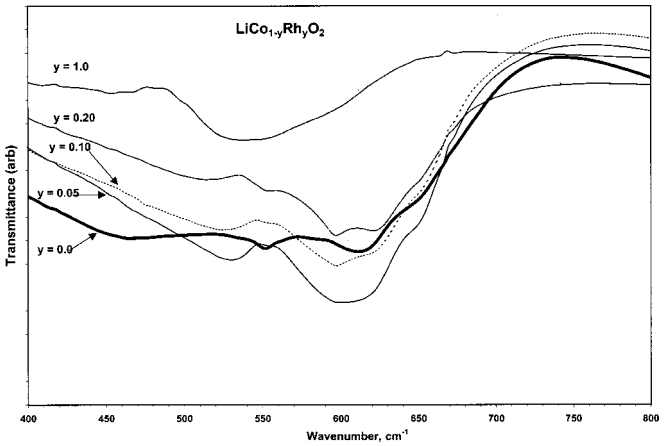

Figure 2. FTIR (transmittance) spectra of the compounds, $LiCo_{1-y}Rh_yO_2$ in the 400-800 cm^{-1} region. y values are indicated.

Our value of RIR for $LiCoO_2$ is 2.67, one of the highest values ever reported, indicating a well-ordered lattice of Li and Co ions in the respective layers (Table I).[8] This value decreases with increasing y in $Li(Co_{1-y}Rh_y)O_2$ and falls to 0.61 for $y = 0.2$. This is much lower than that of $LiRhO_2$ (our value is 0.85; value from the JCPDS file is 1.11[37]), showing that cation disorder exists for $y = 0.20$. Clear splitting of the (006), (102), and (108), (110) doublet peaks in the XRD patterns of the system $Li(Co_{1-y}Ni_y)O_2$ was also considered to be an indication of the absence of cation disorder (cation mixing).[8,10] But, this argument cannot be used for the $Li(Co_{1-y}Rh_y)O_2$ system, due to large difference in the a and c values of the end members (Table I). Thus, while the $y = 0.2$ composition has cation disorder, those with $y = 0.05$ and 0.10 are relatively free of this and can be considered to be ''clean'' phases. However, the IR and electrochemical studies (discussed later) do reveal that for $y = 0.10$, the Rh ions are not randomly distributed in the Co layers and ordering and clustering of Co and Rh ions is occurring. This indicates that the solubility range of Rh ions in the lattice may be $y \leqslant 0.05$ under the synthesis conditions presently employed. Chemical precursor techniques may help in enhancing the solid solubility to higher y values.

Infrared (IR) and Raman spectra have been used to characterize $LiCoO_2$, $LiNiO_2$, and their various solid solutions in the literature.[38-43] Factor group analysis based on the crystal symmetry of the above layer-type compounds predicts four IR-active ($2A_{2u} + 2E_u$) and two Raman active ($A_{1g} + E_g$) vibrational modes.[40,41] The IR modes correspond mainly to the vibrations involving the atomic motion of cations against their oxygen neighbors with the octahedral coordination. Nazri *et al.*[40] have identified these four IR bands in $LiCoO_2$ at 269, 420, 539, and 602 cm^{-1}, whereas Huang and Frech[41] reported the bands at 271, 537, 595, and 653 cm^{-1}. The 653 cm^{-1} band was a shoulder band. The low frequency band situated at 269-270 cm^{-1} was identified as due to the asymmetric stretching vibration of LiO_6 units whereas the three bands in the region 400-600 cm^{-1} correspond to the CoO_6 stretching and bending vibrations. The FTIR spectra in the range 400-800 cm^{-1} for $LiCo_{1-y}Rh_yO_2$ ($y = 0.00$-0.20) and $LiRhO_2$ ($y = 1.0$) are shown in Fig. 2 and the bands are listed in Table I. No distinct peaks were observed in the region 700-4000 cm^{-1} for all the compounds. We have not measured the spectra in the far IR region (150-350 cm^{-1}). Band positions reported in Ref. 40 and 41 for $LiCoO_2$ are also listed in Table I for comparison. In general, only broad bands have been observed for the compounds in the range 400-800 cm^{-1} due to the highly covalent nature of the Co(Rh)-O bonds as compared to the sharp band noted at 270 cm^{-1} in far IR region.[40,41] In $LiCoO_2$, we observed bands at 550 cm^{-1}, a broad band at 610-620 cm^{-1}, and distinct shoulder (sh) band at 655 cm^{-1}. Doping with rhodium ($y = 0.05$-0.20) shifts these bands toward lower wavenumber as can be expected from the relative masses of Co and Rh atoms and their effective reduced masses. However, the broad band observed in the region 595-615 cm^{-1} for $y = 0.05$, splits into two discernable bands at 595 and 625 cm^{-1} for $y = 0.10$ and 0.20. This possibly indicates ordering of the Co and Rh ions in the lattice. The spectrum of $LiRhO_2$ shows only a broad band extending from 525-555 cm^{-1} and a weak shoulder around 600 cm^{-1}. These bands can be assigned to the Rh-O stretching and bending vibrations.

The observed XPS spectra at high resolution for $LiCoO_2$, $Li(Co_{0.9}Rh_{0.1})O_2$ and $LiRhO_2$ were curve fitted and deconvolution was done in cases where necessary. Calibration was done using C 1s peak of 284.6 eV. The spectra are shown in Fig. 3 and the binding energies (BE) are listed in Table II. The O 1s spectrum in $LiCoO_2$ can be deconvoluted to give two peaks (A and B in Fig. 2a) with BEs at 528.9 and 531.3 eV. Peak A can be assigned to O 1s in $LiCoO_2$ in good agreement with the values of 529.0 and 529.6 eV reported for $LiCoO_2$ by Elp *et al.*,[44] and Galakhov *et al.*,[45] respectively. This is also comparable with the value 528.9 eV reported by Mansour[46] in the isostructural compound, $LiNiO_2$. The peak B with a BE of 531.3 eV is assigned to the O 1s in Li_2CO_3 which compares well with the value of 531.7 eV observed by Mansour[46] who observed it as a surface impurity along with $LiNiO_2$. Even though we have not detected Li_2CO_3 impurity in the $LiCoO_2$ by XRD, it is seen in the XPS spectrum because of the high sensitivity of the latter technique. The deconvoluted O 1s peaks (C and D in Fig. 3a) in $LiRhO_2$ occur at 529.6 and 531.2 eV, respectively. Peak C can be assigned to the oxygen in $LiRhO_2$ whereas peak D is due to Li_2CO_3 impurity.

The Rh-doped composition, $LiCo_{0.9}Rh_{0.1}O_2$ also is found to contain two O 1s peaks, (not shown) with the BEs of 528.2 and 531.2 eV corresponding to that of the compound and Li_2CO_3 impurity, respectively (Table II). The difference in the BEs of O 1s in $LiCoO_2$ and $LiRhO_2$ is a reflection of the covalency of the Co-O and Rh-O bonds. This is so due to the fact that these compounds are isostructural with a common Li atom and there is only one type of oxygen atom (6c position in the space group, $R\bar{3}m$). A higher BE of O 1s in $LiRhO_2$ compared to $LiCoO_2$, indicates a less covalent Rh-O bond compared to the Co-O bond. Accordingly, we expect more covalent Li-O bond in $LiRhO_2$ and a lower BE for Li 1s compared to that in $LiCoO_2$. As can be seen from Table II, the BE of Li 1s in $LiCoO_2$ is higher than that in $LiRhO_2$. Interestingly, the BE of Li 1s in 10% Rh-doped compound is higher, by 1.3 eV compared to that of $LiCoO_2$. This higher ionicity of the Li-O bond is indirectly reflected in the increased mobility of Li ions in the lattice. The BE of 53.3 eV for Li 1s in $LiCoO_2$ compares well with the values of 53.7 eV reported by Mansour[46] for $LiNiO_2$. The Co $2p_{3/2}$ spectrum shows a BE of 779.5 eV in $LiCoO_2$, and it gets shifted to 779.3 eV in the 10% Rh-doped compound. The intensity of the peak is also reduced (Table II and Fig. 3b). Our values compare very well with that of 779.9 eV reported by Galakhov *et al.*[45] The Rh $3d_{5/2}$ and Rh $3d_{3/2}$ peaks in $LiRhO_2$ occur at 308.3 and 313.0 eV, respectively (Fig. 3c and Table II). These BEs may be compared with the values of 308-309 eV reported[47] for Rh_2O_3 where the Rh^{3+} ion is in sixfold oxygen coordination with the α-Al_2O_3 structure. As can be expected, the relative intensities of the peaks are smaller for the doped system with $y = 0.1$ and the BEs get shifted by 0.1-0.2 eV as compared to $y = 1.0$ (Fig. 3 and Table II).

Cyclic voltammetry.—Cyclic voltammograms (I-V curves) have been recorded for the various cathodic compositions, $LiCo_{1-y}Rh_yO_2$ ($0.0 \leqslant y \leqslant 0.10$ and $y = 1.0$), using coin-type cells with Li metal as the reference and counter electrode to reveal the phase transitions taking place during the charge/discharge process. Representative I-V curves are shown in Fig. 4. The oxidation and reduction peaks in the I-V curves, respectively, indicate the voltage range in which Li

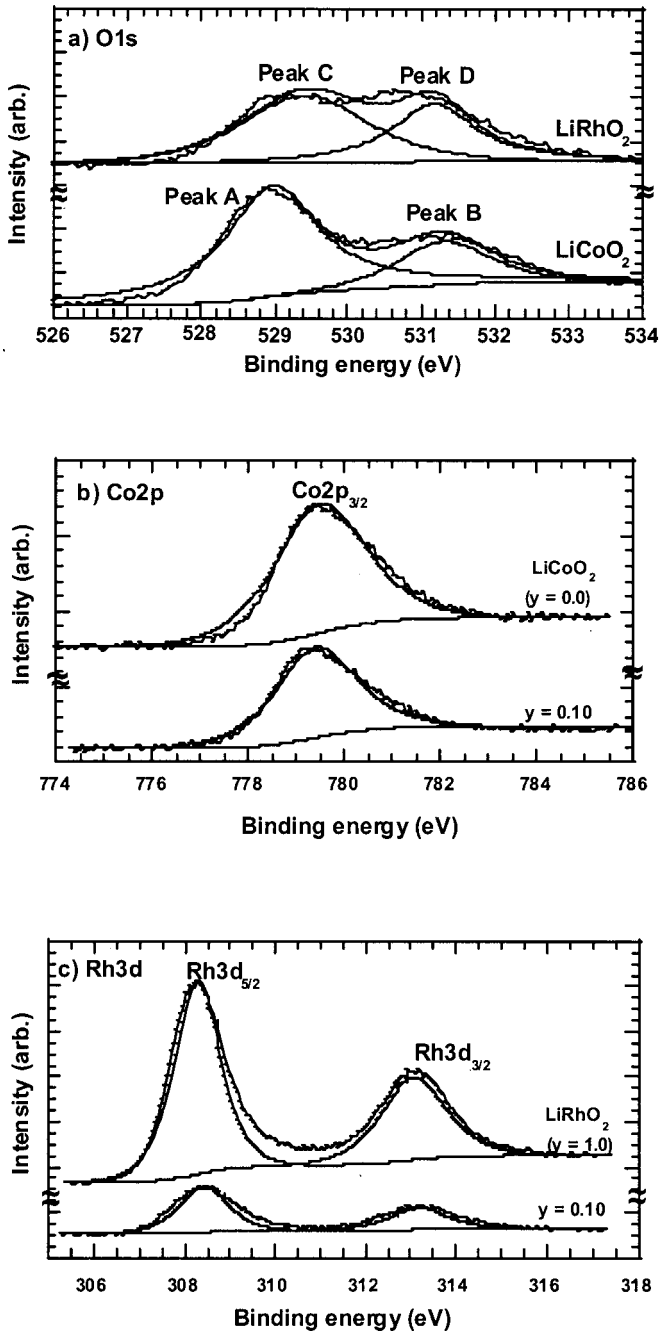

Figure 3. XPS spectra of $LiCo_{1-y}Rh_yO_2$: (a) O 1s in $y = 0.0$ and 1.0, (b) Co 2p in $y = 0.0$ and 0.10, (c) Rh 3d in $y = 0.10$ and 1.0.

deintercalation and intercalation occurs in the compounds. Existence of sharp peaks indicates first-order phase transitions in the compound and two-phase coexistence of two Li-intercalated compositions. Broad and smooth curves in the anodic and cathodic I-V plots indicate either a second-order phase transition or continuous single phase Li deintercalation/intercalation reactions in the oxide materials. In the pristine $LiCoO_2$ ($y = 0.0$), the first cycle anodic curve shows two distinct peaks, one broad peak in the range 4.0-4.15 V (*vs.* Li) indicating a single-phase deintercalation and a small but sharp peak at 4.2 V corresponding to the well-known hexagonal-monoclinic crystallographic phase transformation occurring at $x = 0.5$ in Li_xCoO_2.[30,32] The corresponding reduction peaks occur at a lower voltage, due to hysteresis effects. During the second and subsequent cycles (recorded up to seven cycles), the main oxidation peak shifts slightly to a higher voltage range and the peak at 4.2 V gets broadened and finally merges with the main oxidation peak. Similar behavior occurs with the reduction peaks. These observed features are in good agreement with the I-V behavior reported in the literature[48,49] and indicate that from the second cycle onward, the charge/discharge process occurs in a reversible manner in the voltage scanning region of 3.5-4.3 V (*vs.* Li metal) as a single-phase reaction (Fig. 4a).

Table II. XPS Binding energies of the compounds $LiCo_{1-y}Rh_yO_2$ ($y = 0.0, 0.10, 1.0$).

Elements	Binding energy (±0.1, eV) $LiCoO_2$	$LiCo_{0.9}Rh_{0.1}O_2$	$LiRhO_2$
O 1s	528.9	528.2	529.6
	531.3[a]	531.2[a]	531.2[a]
Li 1s	53.3	54.6	48.1
Co $2p_{3/2}$	779.5	779.3	—
Rh $3d_{5/2}$	—	308.4	308.3
Rh $3d_{3/2}$		313.2	313.0

[a] Corresponds to O 1s binding energy value in Li_2CO_3.

The cyclic voltammograms of the Rh-doped compounds, $y = 0.05$ and 0.10 shown in Fig. 4b and c show distinct changes as compared to $LiCoO_2$. The first cycle I-V curve for $y = 0.05$ shows one broad oxidation peak occurring at 3.98-4.00 V which is lower than the value noted for $y = 0.0$. The 4.2 V peak is either broadened or suppressed in the Rh-doped compound as compared to pristine $LiCoO_2$. These features are essentially unchanged during the second to seventh cycles, including the reduction peaks occurring at 3.85 V (*vs.* Li metal). Significantly, there is a decrease in the hysteresis between the main oxidation and reduction peak voltages as compared to $LiCoO_2$ indicating a better reversibility of the electrode with the composition $y = 0.05$. This is indeed reflected in the charge/discharge cycling behavior to be described later. The I-V curve of the phase with $y = 0.10$ essentially retains the features of the $y = 0.05$ sample with respect to the main oxidation and reduction peaks and the voltage ranges (Fig. 4c). In addition, distinct oxidation peaks occur at 4.09 and 4.20 V and the associated reduction peaks with a hysteresis. The 4.2 V peak is reminiscent of the behavior of $LiCoO_2$ ($y = 0.0$), possibly indicating that in the $y = 0.10$ composition, the distribution of Rh ions in the Co layer is not uniform (*i.e.*, nonrandom) and clustering of Co and Rh ions might have occurred during high temperature synthesis. This is corroborated by the IR data, the unusually low values of the hexagonal *a* and *c* lattice parameters (Table I and Fig. 2), and the galvanostatic charging curves described later. Nevertheless, existence of the peaks indicates the phase transitions in the compound at these voltage values and that these are reversible with respect to Li deintercalation and intercalation. These occur at $x < 0.5$ in $Li_x(Co_{0.9}Rh_{0.1})O_2$ and indicates either ordering of the (Co-Rh) ions and/or the Li vacancies in their respective layers. This is in addition to any disorder or clustering of the ions in their respective layers introduced during high temperature synthesis of the compounds.

The I-V curves of $LiRhO_2$ ($y = 1.0$) are shown in Fig. 4d. The main oxidation peak was observed at 3.70-3.75 V in the anodic region preceded by a small shoulder peak at 3.65-3.70 V. In addition to the main oxidation peak, three other low intensity oxidation peaks are observed at 3.25, 3.35, and 3.9-4.0 V. The corresponding reduction peaks occur at a lower voltage due to hysteresis effects. This is a clear indication of several reversible phase transitions occurring in the $LiRhO_2$ crystal lattice during Li deintercalation and intercalation. These phase transitions must be due to the ordering of Li ions in the Li layer and/or Rh ions (in the Rh layer) in the crystal lattice at fixed values of *x* in Li_xRhO_2 ($x < 1.0$). Similar type of crystal-

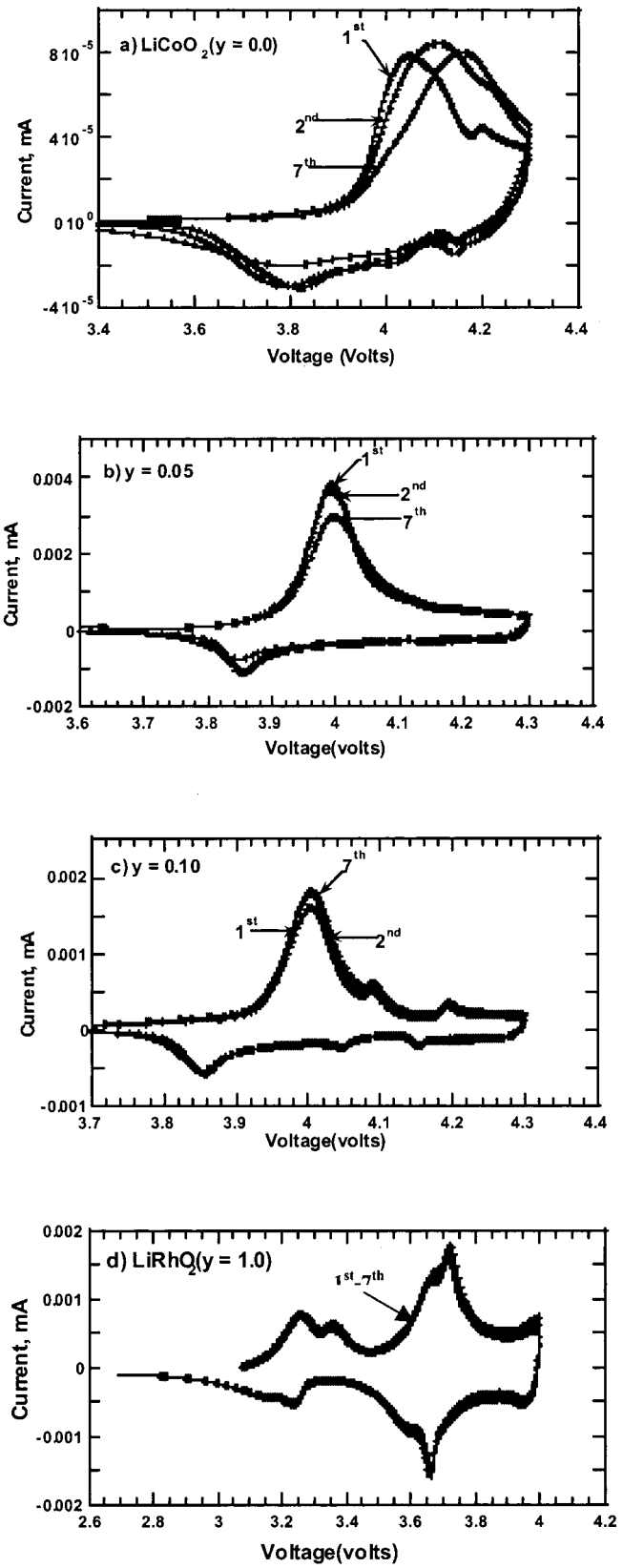

Figure 4. Cyclic voltammograms for the compounds $LiCo_{1-y}Rh_yO_2$ (y = 0.0, 0.05, 0.10 and 1.0). Coin-type cell with Li metal as reference/counter electrode. Scan rate, 0.05 mV/s.

lographic phase transitions are well known to occur in Li_xNiO_2 ($0 < x < 1.0$).[31,50,51] However, the low intensity of the peaks as compared to the main oxidation and reduction peaks in the cyclic voltammograms indicates that the extent of departure from the original hexagonal layer structure is small. In any case it would be interesting to establish the crystal symmetry of these Li_xRhO_2 phases. Another interesting feature observed in the $LiRhO_2$ is that the I-V curves (first to seventh cycles) overlap exactly without any shift in the voltage values during cycling as can be seen in the Fig. 4d.

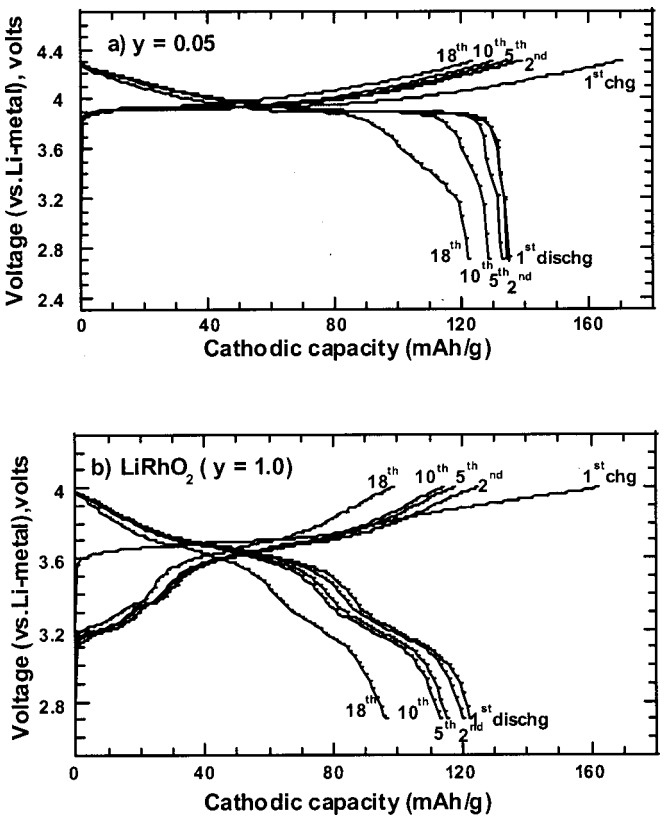

Figure 5. Representative charge/discharge curves of the compounds, $LiCo_{1-y}Rh_yO_2$ (y = 0.05 and 1.0) at 0.14C rate. Voltage window: 2.7-4.3 V for y = 0.05 and 2.7-4.0 V for y = 1.0.

Cathodic behavior and galvanostatic charge/discharge cycling.—Galvanostatic charge/discharge curves have been recorded for $LiCo_{1-y}Rh_yO_2$ cathode materials at 0.14C (1C = 140 mAh/g) up to 18 cycles in the voltage window 2.7-4.3 V for $y \leqslant 0.10$ and 2.7-4.0 V for $LiRhO_2$. The data are presented in Table I. Representative charge/discharge curves of y = 0.05 and 1.0 are shown in Fig. 5. All the compounds showed an irreversible capacity loss between the first charge and first discharge. Pristine $LiCoO_2$ (y = 0.0) showed an irreversible loss of only 15 mAh/g while y = 0.05 and 0.10 compositions and $LiRhO_2$(y = 1.0) showed irreversible losses of 35, 17, and 40 mAh/g, respectively, in the first charge/discharge cycle. From the second cycle onward, the charge and discharge capacities are almost the same (±1%) indicating good reversibility of the materials for all values of y. This is evident from Fig. 5 where the curves for composition with y = 0.05 indicate the suppression of the phase transitions (present in $LiCoO_2$; not shown) and a single phase nature of the Li deintercalation/intercalation process at reduced voltage ranges. Note the behavior of $LiRhO_2$ (y = 1.0): even though exhibiting plateaus in the charge/discharge curves, shows excellent reversibility at 0.14C rate in the 2.7-4.0 V voltage window.

The discharge capacity at the 0.14C rate as a function of number of cycles for various compositions of y in $LiCo_{1-y}Rh_yO_2$ is shown in Fig. 6. The capacity retention, as a percent of the initial discharge

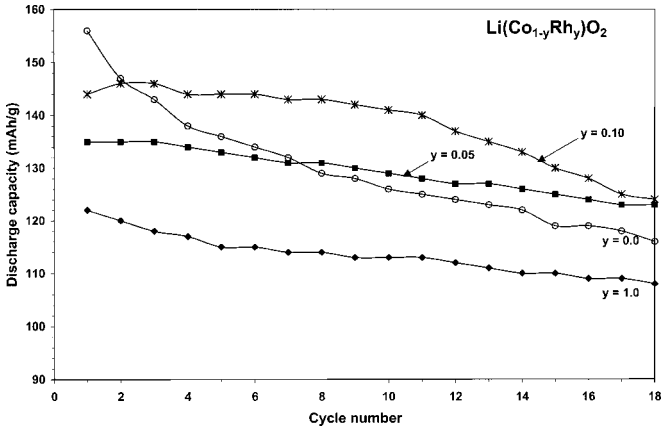

Figure 6. Discharge capacity *vs.* number of charge/discharge cycles for the compounds, $LiCo_{1-y}Rh_yO_2$ at 0.14C rate. y values indicated. Voltage window: 2.7-4.3 V for $0.0 \leqslant y \leqslant 0.10$ and 2.7-4.0 V for $y = 1.0$.

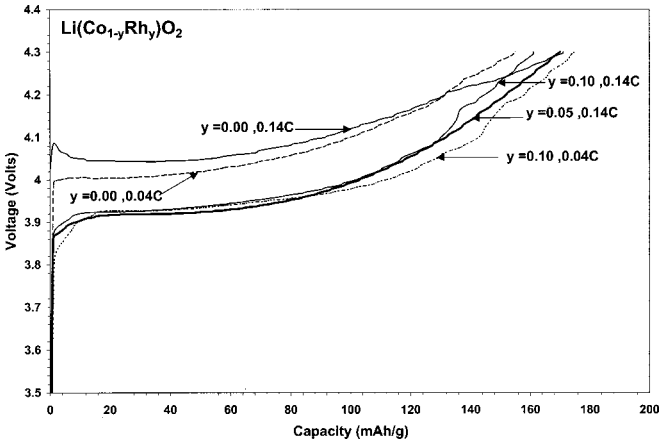

Figure 7. Galvanostatic charging curves of the compounds, $LiCo_{1-y}Rh_yO_2$ at two different current ratings: $y = 0.0$, 0.05, 0.10 (0.14C rate) and $y = 0.0$, 0.10 (0.04C rate) in the voltage window 2.7-4.3 V (*vs.* Li).

capacity, is presented in Table I. We have not examined the behavior at higher current ratings or up to extended number cycles for the obvious reason that rhodium, being a precious metal, is not a commercially viable element as a dopant to improve the cathodic behavior of $LiCoO_2$. Nevertheless, Fig. 6 shows that Rh doping has a beneficial effect in suppressing the phase transitions and capacity fading in $LiCoO_2$. The $y = 0.05$ composition exhibits better electrochemical performance and a capacity retention of 91% as compared to the $y = 0.10$ composition (86%), although the latter shows consistently higher capacity up to at least 10 cycles. More importantly, $LiRhO_2$ has a much better charge/discharge cycling behavior retaining as much as 90% of the initial discharge capacity after 18 cycles (Table I and Fig. 6). On the other hand, the cathodic performance of the isostructural analogues, $LiFeO_2$[12] and $LiCrO_2$[21] were found to be very poor. Also, the performance of $LiCo_{0.95}Rh_{0.05}O_2$ (M = Rh: $y = 0.05$) is much better than that of other trivalent ion-doped $LiCoO_2$ reported in the literature (M = Fe: $y \leqslant 0.24$;[22] M = B: $y = 0.05$;[23] M = Al: $y \leqslant 0.25$[24-27]). The above results are in agreement with the cyclic voltammetric I-V curves described earlier with respect to the suppression of phase transitions in $LiCoO_2$ by the Rh dopant and the existence of phase transitions in $LiRhO_2$ during chargedischarge process. In earlier studies, changes in the intercalation voltage have been observed in solid solutions, $Li(Co_{1-y}Al_y)O_2$ ($y < 0.50$)[24-27] and $Li(Co_{1-y}Ni_y)O_2$ ($0 \leqslant y \leqslant 1$),[6,7,52] where complete solid solubility of the dopant ion has been established. A close examination of Fig. 6 in Ref. 22 also indicates a change (reduction) in the deintercalation voltage in the system $Li(Co_{1-y}Fe_y)O_2$ ($y < 0.24$). Available literature data on $Li(Co_{1-y}Al_y)O_2$ also show that the increase in the deintercalation voltage is directly proportional to the dopant concentration (y).[24,25,53] In our studies on the $Li(Co_{1-y}Rh_y)O_2$ system, clear indication of reduction in the deintercalation voltage for $y = 0.05$, as compared to $y = 0.0$ is obtained from the I-V curves shown in Fig. 4a and b. In order to more clearly discern the effect for compositions, $y = 0.0$, 0.05, and 0.10, galvanostatic charging curves at both 0.14 and 0.04C have been recorded, and the data are shown in Fig. 7. The curve for $y = 0.05$ at 0.14C is an expanded version of the first-charge curve given in Fig. 5. The deintercalation voltages at 0.04C (for a given capacity), for $y = 0.00$ and 0.10 are slightly lower than that noted at 0.14C, though it is more clearly seen for $y = 0.00$. For a capacity of 40 mAh/g, corresponding to $x \approx 0.15$ in $Li_{1-x}(Co_{1-y}Rh_y)O_2$, the deintercalation voltages at 0.14C for $y = 0.00$, 0.05, and 0.10 are 4.05, 3.93, and 3.92 V (*vs.* Li metal), respectively. Thus, there is a decrease of 0.12 V between $y = 0.00$ and 0.05 compositions. A similar trend is also seen for compositions $y = 0.00$ and 0.10 recorded at 0.04C (Fig. 7). However, there is no further appreciable decrease in the deintercalation voltage between the compositions $y = 0.05$ and 0.10. A possible reason for this behavior is that the decrease in the voltage is not a linear function of the dopant concentration (y), or there may be a clustering/ordering of Co/Rh ions in the Co layer for the $y = 0.10$ composition, as compared to the case when $y = 0.05$ where the Co and Rh ions are randomly distributed in the Co layer in the lattice. Evidence for the latter argument was seen in the IR and I-V data, as discussed earlier. Thus, the effect of an increase in y from 0.05 to 0.10 in $Li(Co_{1-y}Rh_y)O_2$ system is not reflected in a further decrease in the deintercalation voltage. Since Rh is a 4d transition metal, the voltage range of 3.2-3.7 V (*vs.* Li) presently noted with respect to Li deintercalation/intercalation in $LiRhO_2$ is slightly more than that encountered in other 4d metal oxides like Nb_2O_5[54] and MoO_3[55] and is in accord with empirical arguments proposed by Ohzuku *et al.*[56] that the operating voltages (*vs.* Li metal) for the metal (di-) oxides vary in the approximate order, 3d > 4d > 5d.

Detailed studies by the group of Delmas[30] and others[48,49,57] have shown that deintercalation of lithium in $LiCoO_2$ brings about extensive changes in its physical properties. The diamagnetic behavior of $LiCoO_2$ arises due to the existence of Co^{3+} in the low-spin state (d^6: $t_{2g}^6e_g^0$). Strong Co-Co bonding, due to short interatomic distances (≡hexagonal *a*-axis), leads to the formation of a filled t_{2g} band separated by an empty e_g band and thus $LiCoO_2$ can be considered to be a d band semiconductor. The charging process (Li deintercalation) leads to the creation of Co^{4+} ions with the low-spin configuration, $t_{2g}^5e_g^0$ and these induce paramagnetism in the compound. For small values of x in $Li_{1-x}CoO_2$, ($0 \leqslant x \leqslant 0.2$), these Co^{4+} ions are localized and act as electronic holes, contributing to p-type semiconduction. In room temperature electronic conductivity, σ increases by two to three orders of magnitude, from 1×10^{-3} S/cm for $x = 0.0$ to ~1 S/cm for $x = 0.05$ with a lowered activation energy for conduction.[30,32] Tukamoto and West[28] found a similar behavior in Mg-doped $LiCoO_2$ (5 atom %) which also induces the Co^{4+} ion formation in the lattice to satisfy the charge neutrality condition to give $Li(Co^{3+}_{1-2y}Co^{4+}_yMg^{2+}_y)O_2$, $y = 0.05$. At and above $x = 0.5$ in $Li_{1-x}CoO_2$, the compound changes over from semiconductor to metal (with $\sigma \sim 10^3$ to 10^4 S/cm) and possibly from paramagnetic to Pauli paramagnetic (T-independent magnetic susceptibility) behavior.[30] Indirect studies by Li-NMR,[30,57,58] IR,[40] Raman,[42] and X-ray absorption spectroscopy[43,59] also confirm the above changes in physical prop-

erties of $Li_{1-x}CoO_2$ as a function of x brought about either by chemical or electrochemical deintercalation.

It has been established that in doped systems of the type, $Li(Co_{1-y}Ni_y)O_2$ (y = 0-1.0)[31] and $Li(Co_{1-y}Fe_y)O_2$ ($y \leqslant 0.24$),[22] the trivalent Ni and Fe ions preferentially oxidize to the 4+ valence state during charging process as compared to the Co^{3+} ions. Hence, we can expect Rh ions also to oxidize to a 4+ valence in the presently studied system, $LiCo_{1-y}Rh_yO_2$ ($y < 0.1$). Increased electronic conductivity as well as appearance of paramagnetism can be expected on Li deintercalation for $y \leqslant 0.2$. In the case of $LiRhO_2$ (y = 1.0), we may expect Pauli paramagnetism and metallic conduction in $Li_{1-x}RhO_2$ for $x \geqslant 0.5$ similar to $Li_{1-x}CoO_2$, since the electronic configurations of Co (3d metal) and Rh (4d metal) ions are the same in the low-spin state and possibly encounter superconductivity analogous to the behavior shown by $Li_{1-x}NbO_2$, $x \approx 0.64$.[60] It may also be possible to stabilize "RhO_2" in the layer structure by chemical and electrochemical soft chemistry techniques starting from $LiRhO_2$ similar to "CoO_2"[61,62] and "NiO_2."[62,63] Detailed physical studies on $Li_{1-x}RhO_2$ ($x \leqslant 1$) are presently underway and will be reported elsewhere.

Conclusions

Rhodium can be substituted at the Co site in $LiCoO_2$ to form uniform solid solutions of the composition $LiCo_{1-y}Rh_yO_2$ ($0.0 < y < 0.10$) as inferred from the powder XRD patterns. Nominal composition with y = 0.20 leads to cation disorder in the lattice and formation of impurity phase ($LiRhO_2$) under the synthesis conditions employed by us. Synthesis techniques using chemical precursor may enhance the solid solubility to higher values of y. The observed trends in the variation of hexagonal lattice parameters have been explained on the basis of the values for y = 0.0 and 1.0 ($LiRhO_2$) and possible role of covalency effects. Infrared spectra of the solid solutions show a systematic shift of the characteristics IR bands to lower wavenumbers with increasing values of y. $LiRhO_2$ shows only a broad absorption band in the region 525-555 cm^{-1} and a shoulder band at 600 cm^{-1}. XPS binding energies have been listed for O 1s, Li 1s, Co 2p, and Rh 3d for the phases $LiCo_{1-y}Rh_yO_2$; y = 0, 0.1, and 1.0. The observed BEs have been compared with those reported in the literature. Cyclic voltammograms and galvanostatic charge/discharge curves at 0.04 and 0.14C show that for y = 0.05, the phase transformation occurring at x = 0.5 in $Li_{1-x}CoO_2$ is suppressed and the deintercalation voltage is decreased. The compositions with y = 0.05 and 0.10 show improved cathodic behavior and discharge capacity retention compared to $LiCoO_2$ (y = 0) at the 0.14C rate in the voltage range 2.7-4.3 V up to 18 charge discharge cycles. Electrochemical studies on $LiRhO_2$ (y = 1.0) indicate that phase transitions occur on charge/discharge cycling (varying x in $Li_{1-x}RhO_2$) in the voltage window 3.2-3.7 V and these are reversible. This compound shows an initial charge capacity of 162 mAh/g when charged to 4.0V (*vs.* Li metal), corresponding to x = 0.85 in $Li_{1-x}RhO_2$. After an initial loss of 40 mAh/g in capacity, the discharge capacity retention corresponds to 90% after 18 cycles with respect to the initial discharge capacity in the voltage window 2.7-4.0 V. The nature of the phase transitions (first or second order) and the crystal structures of the $Li_{1-x}RhO_2$ phases are yet to be determined. We may expect interesting changes in physical properties in $Li_{1-x}RhO_2$ as a function of x as exhibited by the isostructural and isoelectronic $Li_{1-x}CoO_2$. It may be possible to stabilize RhO_2 in the layer structure similar to CoO_2 and NiO_2 by electrochemical charging to higher voltages. The above studies are in progress.

Acknowledgments

The authors thank Dr. H. J. Lindner for his interest in the progress of the work. Thanks are also due to Doreen Lai and Rasid Ali (IMRE) for technical support.

References

1. M. Broussely, P. Biensan, and B. Simon, *Electrochim. Acta*, **45**, 3 (1999).
2. R. Koksbang, J. Barker, H. Shi, and M. Y. Saidi, *Solid State Ionics*, **84**, 1 (1996).
3. T. Ohzuku, A. Ueda, and M. Nagayama, *J. Electrochem. Soc.*, **140**, 1862 (1993).
4. C. Delmas, J. P. Peres, A. Rougier, A. Demourgues, F. Weill, A. Chadwick, M. Broussely, F. Perton, Ph. Biensan, and P. Willmann, *J. Power Sources*, **68**, 120 (1997).
5. J. P. Peres, F. Weill, and C. Delmas, *Solid State Ionics*, **116**, 19 (1999).
6. C. Delmas, I. Saadoune, and A. Rougier, *J. Power Sources*, **43**, 595 (1993).
7. I. Saadoune and C. Delmas, *J. Mater. Chem.*, **6**, 193 (1996).
8. J. Cho, G. Kim, and H. S. Lim, *J. Electrochem. Soc.*, **146**, 3571 (1999).
9. C. Delmas, M. Menetrier, L. Croguennec, I. Saadoune, A. Rougier, C. Pouillerie, G. Prado, M. Grune, and L. Fournes, *Electrochim. Acta*, **45**, 243 (1999).
10. J. Cho, H. S. Jung, Y. C. Park, G. B. Kim, and H. S. Lim, *J. Electrochem. Soc.*, **147**, 15 (2000).
11. S. Madhavi, G. V. Subba Rao, B. V. R. Chowdari, and S. F. Y. Li, *J. Power Sources*, **93**, 156 (2001).
12. R. Kanno, T. Shirane, Y. Inaba, and Y. Kawamoto, *J. Power Sources*, **68**, 145 (1997).
13. Y. Sakurai, H. Arai, S. Okada, and J. Yamaki, *J. Power Sources*, **68**, 711 (1997).
14. T. Shirane, R. Kanno, Y. Kawamoto, Y. Takeda, M. Takano, T. Kamiyama, and F. Izumi, *Solid State Ionics*, **79**, 227 (1995).
15. B. Fuchs and S. Kemmler-Sack, *Solid State Ionics*, **68**, 279 (1994).
16. Y. Nitta, M. Nagayama, H. Miyabe, and A. Ohta, *J. Power Sources*, **81-82**, 49 (1999).
17. G. Pistoia, A. Antonini, and D. Zane, *Solid State Ionics*, **78**, 115 (1995).
18. A. R. Armstrong and P. G. Bruce, *Nature*, **381**, 499 (1996).
19. P. G. Bruce, A. R. Armstrong, and R. L. Gitzendanner, *J. Mater. Chem.*, **9**, 193 (1999).
20. R. Stoyanova, E. Zhecheva, and I. Zarkova, *Solid State Ionics*, **73**, 233 (1994).
21. C. D. W. Jones, E. Rossen, and J. R. Dahn, *Solid State Ionics*, **68**, 65 (1994).
22. H. Kobayashi, H. Shigemura, M. Tabuchi, H. Sakaebe, K. Ado, H. Kageyama, A. Hirano, R. Kanno, M. Wakita, S. Morimoto, and S. Nasu, *J. Electrochem. Soc.*, **147**, 960 (2000).
23. R. Alcantara, P. Lavela, J. L. Tirado, R. Stoyanova, and E. Zhecheva, *J. Solid State Chem.*, **134**, 265 (1997).
24. G. Ceder, Y-M. Chiang, D. R. Sadoway, M. K. Aydinol, Y. I. Jang, and B. Huang, *Nature*, **392**, 694 (1998).
25. Y. I. Jang, B. Huang, H. Wang, D. R. Sadoway, G. Ceder, Y. M. Chiang, H. Liu, and H. Tamura, *J. Electrochem. Soc.*, **146**, 862 (1999).
26. H. Huang, G. V. Subba Rao, and B. V. R. Chowdari, *J. Power Sources*, **81**, 690 (1999).
27. W. Yoon, K. K. Lee, and K. B. Kim, *J. Electrochem. Soc.*, **147**, 2023 (2000).
28. H. Tukamoto and A. R. West, *J. Electrochem. Soc.*, **144**, 3164 (1997).
29. I. Saadoune, M. Menetrier, and C. Delmas, *J. Mater. Chem.*, **7**, 2505 (1997).
30. M. Menetrier, I. Saadoune, S. Levasseur, and C. Delmas, *J. Mater. Chem.*, **9**, 1135 (1999).
31. C. Delmas, M. Menetrier, L. Croguennec, S. Levasseur, J. P. Peres, C. Pouillerie, G. Prado, L. Fournes, and F. Weill, *Int. J. Inorg. Mater.*, **1**, 11 (1999).
32. S. Levasseur, M. Menetrier, E. Suard, and C. Delmas, *Solid State Ionics*, **128**, 11 (2000).
33. G. Ceder, M. K. Aydinol, and A. F. Kohan, *Comput. Mater. Sci.*, **8**, 161 (1997).
34. A. Mendiboure, H. Eickenbusch, R. Schollhorn, and G. V. Subba Rao, *J. Solid State Chem.*, **71**, 19 (1987).
35. R. D. Shannon, *Acta Crystallogr., Sect. A: Cryst. Phys., Diffr., Theor. Gen. Crystallogr.*, **32A**, 751 (1976).
36. E. J. Wu, P. D. Tepesch, and G. Ceder, *Philos. Mag., B*, **77**, 1039 (1998).
37. JCPDS: Card number 42-0115.
38. T. A. Hewston and B. L. Chamberland, *J. Phys. Chem. Solids*, **48**, 97 (1987).
39. T. Ohzuku, A. Ueda, M. Nagayama, Y. Iwakoshi, and H. Komori, *Electrochim. Acta*, **38**, 1159 (1993).
40. M. Nazri, M. D. Curtis, B. Yabka, G. A. Nazri, and C. Julien, Abstract 48, The Electrochemical Society Meeting Abstracts, Vol. 98-1, San Diego, May 3-8, 1998.
41. W. Huang and R. Frech, *Solid State Ionics*, **86-88**, 395 (1996).
42. M. Inaba, Y. Iriyama, Z. Ogumi, Y. Todzuka, and A. Tasaka, *J. Raman Spectrosc.*, **28**, 613 (1997).
43. S. G. Kang, S. Y. Kang, K. S. Ryu, and S. H. Chang, *Solid State Ionics*, **120**, 155 (1999).
44. J. V. Elp, J. L. Wieland, H. Eskes, P. Kuiper, and G. A. Sawatzky, *Phys. Rev. B*, **44**, 6090 (1991).
45. V. R. Galakhov, E. Z. Kurmaev, St. Uhlenbrock, M. Neumann, D. G. Kellerman, and V. S. Gorshkov, *Solid State Commun.*, **99**, 221 (1996).
46. A. M. Mansour, *Surf. Sci. Spectra*, **3**, 279 (1996).
47. J. F. Moulder, W. F. Stickle, P. E. Sobol, and K. D. Bomben, *Handbook of X-Ray Photoelectron Spectroscopy*, Perkin-Elmer Corp., Eden Prarie, MN (1992).
48. Y-M. Choi and S-I. Pyun, *Solid State Ionics*, **99**, 173 (1997).
49. B. Huang, Y-I. Jang, Y-M. Chiang, and D. R. Sadoway, *J. Appl. Electrochem.*, **28**, 1365 (1998).
50. Y. Gao, M. V. Yakovleva, and W. B. Ebner, *Electrochem. Solid-State Lett.*, **1**, 117 (1998).
51. A. Yu, G. V. Subba Rao, and B. V. R. Chowdari, *Solid State Ionics*, **135**, 131 (2000).
52. C. Delmas and I. Saadoune, *Solid State Ionics*, **53-56**, 370 (1992).
53. Y.-I. Jang, B. Huang, H. Wang, G. R. Maskaly, G. Ceder, D. R. Sadoway, Y.-M. Chiang, H. Liu, H. Tamura, *J. Power Sources*, **81-82**, 589 (1999).

54. N. Kumagai, Y. Koishikawa, S. Komaba, and N. Koshiba, *J. Electrochem. Soc.*, **146**, 3203 (1999).
55. Y. Iriyama, T. Abe, M. Inaba, and Z. Ogumi, *Solid State Ionics*, **135**, 95 (2000).
56. T. Ohzuku, *Proceedings of Trends in Materials Science Conference*, S. Radhakrishna, Editor, p. 1, Malaysia (1997).
57. M. Imanishi, M. Fujiyoshi, Y. Takeda, O. Yamamoto, and M. Tabuchi, *Solid State Ionics*, **118**, 121 (1999).
58. B. Ouyang, X. Cao, H. W. Lin, S. Slane, S. Kostov, M. denBoer, and S. G. Greenbaum, *Mater. Res. Soc. Symp. Proc.*, **369**, 59 (1995).
59. I. Nakai, K. Takahashi, Y. Shiraishi, and T. Nagayama, *J. Phys. IV*, **C2**, 1243 (1997).
60. M. J. Geselbracht, T. J. Richardson, and A. M. Stacy, *Nature*, **345**, 324 (1990).
61. G. G. Amatucci, J. M. Tarascon, and L. C. Klein, *J. Electrochem. Soc.*, **143**, 1114 (1996).
62. L. Seguin, G. Amatucci, M. Anne, Y. Anne, Y. Chabre, P. Strobel, J. M. Tarascon, and G. Vaughan, *J. Power Sources*, **81-82**, 604 (1999).
63. L. Croguennec, C. Pouillerie, and C. Delmas, *J. Electrochem. Soc.*, **147**, 1314 (2000).